

Towards a warped inflationary brane scanning

Heng-Yu Chen*

Department of Physics, University of Wisconsin-Madison, Madison, WI 53706-1390, USA

Jinn-Ouk Gong†

Instituut-Lorentz for Theoretical Physics, Universiteit Leiden, 2333 CA Leiden, The Netherlands

We present a detailed systematics for comparing warped brane inflation with the observations, incorporating the effects of both moduli stabilization and ultraviolet bulk physics. We explicitly construct an example of the inflaton potential governing the motion of a mobile D3 brane in the entire warped deformed conifold. This allows us to precisely identify the corresponding scales of the cosmic microwave background. The effects due to bulk fluxes or localized sources are parametrized using gauge/string duality. We next perform some sample scanings to explore the parameter space of the complete potential, and first demonstrate that without the bulk effects there can be large degenerate sets of parameters with observationally consistent predictions. When the bulk perturbations are included, however, the observational predictions are generally spoiled. For them to remain consistent, the magnitudes of the additional bulk effects need to be highly suppressed.

PACS numbers: 98.80.Cq, 11.25.Mj

CONSTRUCTING A POTENTIAL FOR WARPED BRANE INFLATION

The inflationary paradigm [1] addresses a number of fine tuning problems of the standard hot big bang cosmology, such as the horizon and the flatness problems. It also predicts a nearly scale invariant power spectrum of the curvature perturbation, which has been verified to high accuracies by the observation of the thermal fluctuations in the cosmic microwave background (CMB) and the large scale structure of the universe [2, 3]. Numerous models of inflation based on effective field theory have been proposed, however, distinct predictions of a given model crucially depend on its ultraviolet completion. To construct a truly predictive inflationary model, it is clearly important to embed it into a consistent microscopic theory of quantum gravity such as string theory.

During the past few years, our understanding of the various ingredients for obtaining string inflation has been significantly expanded, and many models with increasing sophistication and striking signatures have been proposed (For recent developments, see Ref. [4] and references therein). In the coming decade, beyond the ongoing Sloan Digital Sky Survey [2] and the Wilkinson Microwave Anisotropy Probe [3], vastly improved cosmological data will become available from the advanced CMB observations [5], the CMB polarization experiments [6], the dark energy surveys [7] as well as the map of large scale structure [8]. They will allow us to constrain the parameter spaces of these models, and possibly to even rule out some of them. It is therefore of timely interest to perform a thoroughly updated and complete case study in such a direction¹. In this paper we shall focus on one of the most

developed string inflation models in the literature, usually referred to as “brane inflation”.

The original setup of brane inflation first introduced in Ref. [9] is to consider a pair of spacetime-filling D3-D $\bar{3}$ branes, separated at some distance greater than the local string length on a compact six manifold. As D3 and D $\bar{3}$ move towards each other under the Coulombic attraction, the canonical inflaton is then identified as the separation between them. Unfortunately in such a simple setup, the Coulombic attraction is too strong for the slow-roll inflation to persist. To overcome this obstacle, the authors of Ref. [10] considered instead placing the D3-D $\bar{3}$ pair in a locally warped deformed conifold throat developed in a compact Calabi-Yau orientifold by background fluxes. The D $\bar{3}$ is then stabilized at the tip of deformed conifold, and D3 is attracted weakly by the warped down D3-D $\bar{3}$ potential given by

$$V_{D3\overline{D3}}(\tau, \sigma) = \frac{D_0}{U^2} \left(1 - \frac{3D_0}{16\pi^2 T_3^2 |\mathbf{y} - \bar{\mathbf{y}}|^4} \right). \quad (1)$$

Here $D_0 = 2T_3 a_0^4$, $T_3 = 1/[(2\pi)^3 g_s (\alpha')^2]$ is the D3 brane tension, $a_0 = \exp[-2\pi K/(3g_s M)]$ is the warp factor at the tip of deformed conifold with $-K$ and M being the quanta of NSNS and RR three form fluxes, and $|\mathbf{y} - \bar{\mathbf{y}}|$ is the D3-D $\bar{3}$ separation. Furthermore, the factor U is the universal Kähler modulus, whose role we shall discuss in detail later. Notice that the first term in (1) gives the positive contribution and uplifts the total potential energy, whereas the Coulombic attraction is highly suppressed by a_0^8 and only becomes dominating near the tip of deformed conifold. Eventually when $|\mathbf{y} - \bar{\mathbf{y}}|$ becomes comparable to warped string length $\sim a_0 l_s$, D3 and D $\bar{3}$ annihilate through open string tachyon condensation, rapidly terminates the brane inflation.

There are two important further ingredients that have so far been missing in our discussion, and they are crucial for obtaining the inflationary phase and making detailed comparisons

¹ What we mean by “complete” should become clear momentarily.

with observational data. The first ingredient is the stabilization of both closed and open string moduli. They are usually stabilized by the perturbative flux potential [11] and the non-perturbative superpotential generated by wrapped branes [12]. The second ingredient is the ultraviolet corrections arising from embedding the warped throat into a compact Calabi-Yau orientifold. The bulk fluxes and the distant branes, or additional supersymmetry breaking and moduli stabilization sources can give significant perturbations to the inflaton potential derived from the local sources and geometry.

The warped deformed conifold offers us an ideal venue to analyze these two ingredients. Its explicit metric [13] allows for studying the moduli stabilization and the construction of the inflaton potential valid for the *entire* evolution, including precise identification of where inflation ends. Furthermore while bulk physics is largely unknown, the spectrum of supergravity states in singular conifold has been tabulated in Ref. [14]. The gauge/string duality then allows us to parametrize these symmetry breaking bulk perturbations to the inflaton potential by coupling dual (approximately) conformal field theory to these bulk modes [15]. Combining these with the D3- $\overline{\text{D3}}$ interaction, we can schematically parametrize the total potential of the inflaton ϕ including both local and bulk effects, experienced by a mobile D3 brane in the warped deformed conifold as

$$\mathbb{V}(\phi) = V_{D3\overline{D3}}(\phi) + V_{\text{stab.}}(\phi) + V_{\text{bulk}}(\phi). \quad (2)$$

Here $V_{\text{stab.}}(\phi)$ arises from moduli stabilization and $V_{\text{bulk}}(\phi)$ encodes all other possible perturbations from bulk physics². Most of the quantities specifying $V_{\text{stab.}}(\phi)$ are exclusively related to the local geometry of the throat, e. g. the warp factor a_0 . However $V_{\text{stab.}}(\phi)$ typically also depends on other quantities controlled by bulk physics, such as the one loop determinant of the non-perturbative superpotential. The quantities controlling $V_{\text{stab.}}(\phi)$ are usually treated as free parameters and yield a landscape of possible inflaton potentials.

The current observational data [2, 3] enable us to make comparisons with the predictions yielded by different parameter sets and constrain their allowed values. In order for this exercise to be instructive, it is crucial to include all the significant contributions to the inflaton potential. The existing literature in this direction [16, 17] has mostly focused on the first two contributions in (2) without taking into account $V_{\text{bulk}}(\phi)$. However in light of recent results in Ref. [15] indicating that $V_{\text{bulk}}(\phi)$ can be generically comparable to $V_{\text{stab.}}(\phi)$, it is clearly necessary to apply such general results and scan the enlarged parameter space to include the bulk corrections.

² Although we follow similar scheme as in Ref. [15], we do not partition $V_{\text{stab.}}(\phi)$ such that the inflaton mass term $\sim H^2\phi^2$ is singled out. As H^2 is usually a combination of microscopic parameters, for the purpose of full parameter scanning we shall calculate $V_{\text{stab.}}(\phi)$ in full detail and express it explicitly in terms of the microscopic parameters while treating $V_{\text{bulk}}(\phi)$ as further perturbations.

Here we aim to provide some initial steps toward a complete systematic parameter scanning for warped brane inflation. We shall first consider a specific brane configuration and stabilize explicitly both universal Kähler modulus and some of the angular moduli of D3. We then construct an example of $V_{D3\overline{D3}}(\phi) + V_{\text{stab.}}(\phi)$ valid for *entire* warped deformed conifold throat. This potential should be regarded as the infrared completion to the model obtained in Ref. [18] under the singular conifold limit (See also [19, 20] for related work). It allows us to identify the end point of inflation, hence extrapolate precisely to the CMB scale. Next we shall briefly review the parametrization of the bulk effects $V_{\text{bulk}}(\phi)$ given in Ref. [15], and discuss the microscopic and observational constraints on the inflationary parameter scanning. Finally we shall first present different degenerate parameter sets such that the resultant $V_{D3\overline{D3}}(\phi) + V_{\text{stab.}}(\phi)$ yields observationally consistent curvature power spectrum $\mathcal{P}_{\mathcal{R}}$ and the corresponding spectral index $n_{\mathcal{R}}$. We next demonstrate that the perturbations due to $V_{\text{bulk}}(\phi)$ can have significant impact and need to be small to preserve these seemingly optimal parameter sets. These sample scanings aim to highlight the possible degeneracies and the important role of bulk effects.

ENUMERATING THE INFLATON POTENTIAL

Moduli stabilization potential from warped throat

In this section, we shall explicitly consider the effects of moduli stabilization on the mobile D3 brane in the entire deformed conifold. This is important for accurate comparisons between the predictions and the observational data. In particular, this allows us to identify *precisely* the end point of inflation ϕ_e , defined to be the point where the slow-roll parameter

$$\epsilon \equiv 2M_{\text{Pl}}^2 \left[\frac{H'(\phi)}{H(\phi)} \right]^2 \approx \frac{M_{\text{Pl}}^2}{2} \left[\frac{\mathbb{V}'(\phi)}{\mathbb{V}(\phi)} \right]^2 \quad (3)$$

becomes 1 so that the universe ceases accelerated expansion. Here, $M_{\text{Pl}} = (8\pi G)^{-1/2}$, $H(\phi)$ is the field dependent Hubble parameter and a prime denotes a derivative with respect to ϕ . Note that the second approximation holds under the slow-roll limit. It is crucial to properly take into account the late evolution of the universe during inflation for making correct inflationary predictions. The form of the potential near the end of inflation can substantially lower the inflationary energy scale [21], and the light fields other than the canonical inflaton can completely dominate the curvature power spectrum $\mathcal{P}_{\mathcal{R}}$ and the corresponding spectral index $n_{\mathcal{R}}$ [22]. Furthermore, the post-inflationary evolution can also modify the spectral index at an observationally detectable level [23].

In the context of warped brane inflation, $\epsilon(\phi)$ is driven towards 1 mostly by the D3- $\overline{\text{D3}}$ Coulombic attraction, which is exponentially suppressed and only becomes significant inside the deformed conifold. Moreover, as shown in Ref. [24] when Coulombic attraction is insignificant, $\epsilon(\phi)$ remains small all

the way to the tip for generic parameter sets. We therefore expect inflation persists well into the deformed conifold region, despite only a proportionally small number of e -folds is expected to be generated there. Moreover as some of the inflationary predictions are already tightly constrained by observations to high degrees of accuracies, e.g. $\mathcal{P}_{\mathcal{R}}$ and $n_{\mathcal{R}}$, it is important to take into account such infrared completion in constraining the parameter space of brane inflation.

The key component capturing the moduli stabilization effects on the mobile D3 is the $\mathcal{N} = 1$ supergravity F -term scalar potential,

$$V_F(z^\alpha, \bar{z}^\alpha, \rho, \bar{\rho}) = e^{\kappa^2 \mathcal{K}} \left(\mathcal{K}^{\Sigma\Omega} D_\Sigma W \overline{D_\Omega W} - 3\kappa^2 |W|^2 \right), \quad (4)$$

where $\kappa^2 = M_{\text{pl}}^{-2}$. Let us discuss various contributions to (4) in turn. In the presence of a D3 brane, the universal Kähler modulus $U(z, \rho)$ depends on the brane position $\{z^\alpha, \bar{z}^\alpha\}$ and the usual complex bulk Kähler modulus $\rho = \sigma + i\chi$. The indices in (4) therefore runs over $\{\rho, z^\alpha\}$ and total Kähler potential is the given by [25]

$$\begin{aligned} \kappa^2 \mathcal{K}(z^\alpha, \bar{z}^\alpha, \rho, \bar{\rho}) &= -3 \log[\rho + \bar{\rho} - \gamma k(z^\alpha, \bar{z}^\alpha)] \\ &\equiv -3 \log U(z, \rho). \end{aligned} \quad (5)$$

Here, $k(z^\alpha, \bar{z}^\alpha)$ is the geometric Kähler potential of the metric on the Calabi-Yau, and $\gamma = \sigma_0 T_3 / (3M_{\text{pl}}^2)$ is the normalization constant with σ_0 being the value of σ when the D3 brane is at its stabilized configuration [18], including the uplifting potentials³.

To stabilize some of the geometric and Kähler moduli, we need to consider the total superpotential $W(z^\alpha, \rho)$ consisting of two contributions as

$$W(z^\alpha, \rho) = W_0 + A(z^\alpha) e^{-a\rho}. \quad (6)$$

The first term $W_0 = \int G_3 \wedge \Omega_3$ is the perturbative flux superpotential [11], which allows us (at least in principle) to stabilize the complex structure moduli and dilaton-axion. One mechanism for stabilizing ρ and some of the mobile D3 brane position moduli is to include non-perturbative effects through gaugino condensation on a stack of space-filling D7 branes (or a Euclidean D3 brane instanton), as appears in the second term of (6). The prefactor $A(z^\alpha)$ is a holomorphic function of the D3 brane moduli and can be written as [28]

$$A(z^\alpha) = A_0 \left[\frac{f(z^\alpha)}{f(0)} \right]^{1/n}. \quad (7)$$

Here A_0 is a complex constant whose exact value depends on the stabilized complex structure moduli, and n is the number of D7 (or $n = 1$ for Euclidean D3) giving the gaugino condensate (or instanton correction). The parameter a in (6) is given

by $2\pi/n$. The explicit dependence on the position of mobile D3 brane appears through the holomorphic embedding function $f(z^\alpha) = 0$ of the four cycle in the Calabi-Yau space.

Substituting the total superpotential (6) as well as the expression for the inverse metric $\mathcal{K}^{\Sigma\Omega}$ solved in Ref. [19] into (4), the explicit form of $V_F(z^\alpha, \bar{z}^\alpha, \rho, \bar{\rho})$ is given by

$$\begin{aligned} V_F(z^\alpha, \bar{z}^\alpha, \rho, \bar{\rho}) &= \frac{\kappa^2}{3[U(z, \rho)]^2} \left\{ \left[U(z, \rho) + \gamma k^{\gamma\delta} k_\gamma k_\delta \right] |W_\rho|^2 - 3(\overline{W} W_\rho + c.c.) \right\} \\ &+ \frac{\kappa^2}{3[U(z, \rho)]^2} \left[\left(k^{\alpha\bar{\delta}} k_{\bar{\delta}} \overline{W}_{,\bar{\rho}} W_{,\alpha} + c.c. \right) + \frac{1}{\gamma} k^{\alpha\bar{\beta}} W_{,\alpha} \overline{W}_{,\bar{\beta}} \right]. \end{aligned} \quad (8)$$

Here, the subscript of a letter with a comma denotes a partial differentiation with respect to the corresponding component. Specifically for a deformed conifold defined by the complex embedding equation $\sum_{\alpha=1}^4 (z^\alpha)^2 = \varepsilon^2$ with $z^\alpha \in \mathbb{C}$, the Kähler potential is given by

$$k(\tau) = \frac{\varepsilon^{4/3}}{2^{1/3}} \int_\tau d\tau' [\sinh(2\tau') - 2\tau']^{1/3}. \quad (9)$$

In writing (9), we have also used the standard relation $\sum_{\alpha=1}^4 |z^\alpha|^2 = \varepsilon^2 \cosh \tau$ (See Refs. [13, 29] for the explicit metric in terms of τ and angular coordinates). To apply the general formula (8), we note the inverse metric $k^{\bar{i}j}$ is given by

$$k^{\bar{i}j} = \frac{r^3}{k''} \left[R^{\bar{i}j} + \coth \tau \left(\frac{k''}{k'} - \coth \tau \right) L^{\bar{i}j} \right], \quad (i, \bar{j} = 1, 2, 3) \quad (10)$$

where $k' = dk/d\tau$ and $k'' = d^2k/d\tau^2$, and the 3×3 matrices $R^{\bar{i}j}$ and $L^{\bar{i}j}$ in (10) are, respectively,⁴

$$R^{\bar{i}j} = \delta^{\bar{i}j} - \frac{z_i \bar{z}_j}{r^3}, \quad (11)$$

$$L^{\bar{i}j} = \left(1 - \frac{\varepsilon^4}{r^6} \right) \delta^{\bar{i}j} + \frac{\varepsilon^2}{r^3} \frac{z_i z_j + \bar{z}_i \bar{z}_j}{r^3} - \frac{z_i \bar{z}_j + \bar{z}_i z_j}{r^3}. \quad (12)$$

We can now readily calculate various terms depending on the inverse deformed conifold metric $k^{\bar{i}j}$ in the F -term scalar potential (8). First we notice that $L^{\bar{i}j}$ has the property $k_i L^{\bar{i}j} = L^{\bar{i}j} k_j = 0$; therefore, the norm $k^{\bar{i}j} k_i k_j$ is given by

$$k^{\bar{i}j} k_i k_j = \frac{3 \varepsilon^{4/3}}{4 \cdot 2^{1/3}} \frac{[\sinh(2\tau) - 2\tau]^{4/3}}{\sinh^2 \tau}. \quad (13)$$

Similarly, we can calculate that

³ Strictly speaking, the derivation of (5) given in Ref. [25] is invalid for the warped background, hence raises the question about the validity of (5) itself in the warped deformed conifold. However, some interesting new development in Ref. [26] about the universal Kähler modulus indicates that (5) can remain valid in the warped background. It would be useful to verify this by

combining the earlier work on the dynamics of warped compactification, e.g. Ref. [27] with the recent results, Ref. [26]. We thank Bret Underwood for discussing with us about this issue.

⁴ Here, we have made the substitution $z_4 = \pm \sqrt{\epsilon^2 - (z_1^2 + z_2^2 + z_3^2)}$.

$$k^{\bar{i}j} k_{\bar{i}} W_j = \frac{3 \cosh \tau}{4 \sinh^3 \tau} [\sinh(2\tau) - 2\tau] \sum_{j=1}^3 \left(z_j - \bar{z}_j \frac{\epsilon^2}{r^3} \right) A_j e^{-\alpha \rho}, \quad (14)$$

$$k^{\bar{i}j} \bar{W}_{\bar{i}} W_j = \frac{3}{2 \cdot 2^{2/3}} \epsilon^{2/3} \frac{\cosh \tau}{\sinh \tau^2} [\sinh(2\tau) - 2\tau]^{2/3} \left\{ R^{\bar{i}j} \bar{W}_{\bar{i}} W_j + \left[\frac{2}{3} \frac{\sinh(2\tau)}{\sinh(2\tau) - 2\tau} - \coth^2 \tau \right] \times L^{\bar{i}j} \bar{W}_{\bar{i}} W_j \right\}, \quad (15)$$

where

$$R^{\bar{i}j} \bar{W}_{\bar{i}} W_j = e^{-2\alpha\sigma} \left[\sum_{i=1}^3 |A_i|^2 - \frac{1}{r^3} \left(\sum_{i=1}^3 z_i \bar{A}_i \right) \left(\sum_{j=1}^3 \bar{z}_j A_j \right) \right], \quad (16)$$

$$L^{\bar{i}j} \bar{W}_{\bar{i}} W_j = e^{-2\alpha\sigma} \left\{ \sum_{i=1}^3 \left(1 - \frac{\epsilon^4}{r^6} \right) |A_i|^2 - \frac{1}{r^3} \left(\sum_{i,j=1}^3 \bar{A}_i \left[z_i \bar{z}_j + z_j \bar{z}_i - \frac{\epsilon^2}{r^3} (z_i z_j + \bar{z}_i \bar{z}_j) \right] A_j \right) \right\}. \quad (17)$$

Putting various components together, we can obtain the general expression of the F -term scalar potential in deformed conifold. We shall see that for a specific D7 embedding given in Ref. [30], the resultant expression nicely simplifies along its angular stable trajectory.

A case study

As an explicit example, we consider specifically the D7 brane embedding given by [30]

$$f(z^\alpha) = z_1 - \mu, \quad (18)$$

from which we can easily find that

$$A(z^\alpha) = A_0 \left(1 - \frac{z_1}{\mu} \right)^{1/n}, \quad (19)$$

$$A_i(z^\alpha) = -\frac{A_0}{n\mu} \left(1 - \frac{z_1}{\mu} \right)^{1/n-1} \delta_{i1}. \quad (20)$$

Without loss of generality, we shall take $\mu \in \mathbb{R}^+$. The embedding (18) is highly symmetric, and preserves $SO(3)$ subgroup of the full $SO(4)$ continuous isometry group of the deformed conifold.⁵ Substituting $A_i(z^\alpha)$ and $\bar{A}_j(z^\alpha)$ into the earlier expressions derived for the F -term scalar potential, the dependence on the D3 brane position now only appears through the combinations $(z_1 + \bar{z}_1)$ and $|z_1|^2$. The resultant expression therefore has the functional dependence $V_F = V_F(z_1 + \bar{z}_1, |z_1|^2, \tau, \sigma, \chi)$.

In addition, we also need to stabilize some of the moduli appearing in $V_F(z_1 + \bar{z}_1, |z_1|^2, \tau, \sigma, \chi)$ following the standard procedure outlined in Ref. [18]. First the axion of the complex Kähler modulus χ can be stabilized by rotating the phase of the flux induced superpotential $W_0 \in \mathbb{R}^-$, and making the replacement $\exp(i\alpha\chi)/A(z^\alpha) \rightarrow 1/|A(z^\alpha)|$. As the isometry of the deformed conifold is partially broken by D7 branes, some of the angular coordinates of the mobile D3 can also be stabilized by the resultant F -term scalar potential. In Ref. [24], such specific angular stable trajectory for the D7 embedding (18) for the entire deformed conifold is derived to be

$$z_1 = -\epsilon \cosh \left(\frac{\tau}{2} \right). \quad (21)$$

We refer the readers to Ref. [24] for the derivation of this trajectory and the discussion about its stability⁶. The resultant two-field scalar potential $V_F(\tau, \sigma)$, for such an angular stable trajectory, is thus given by

$$V_F(\tau, \sigma) = \frac{2a^2 \kappa^2 |A_0|^2 e^{-2\alpha\sigma}}{[U(\tau, \sigma)]^2} |g(\tau)|^{2/n} \times \left\{ \frac{U(\tau, \sigma)}{6} + \frac{1}{a} \left(1 - \frac{|W_0|}{|A_0|} \frac{e^{\alpha\sigma}}{[g(\tau)]^{1/n}} \right) + F(\tau) \right\}, \quad (22)$$

⁵ The actual angular stable trajectory however only preserves $SO(2)$ subgroup of $SO(3)$.

⁶ Furthermore, as the angular dependences are only encoded in the F -term scalar potential (at least for the region where most of e -folds occur), we expect including the uplifting term does not affect the stability analysis.

where various functions in V_F are

$$U(\tau, \sigma) = 2\sigma - \gamma k(\tau), \quad (23)$$

$$g(\tau) = 1 + \frac{\varepsilon}{\mu} \cosh\left(\frac{\tau}{2}\right), \quad (24)$$

$$F(\tau) = \varepsilon^{4/3} \gamma \left[K(\tau) \sinh\left(\frac{\tau}{2}\right) \right]^2 \times \left[K(\tau) \cosh\left(\frac{\tau}{2}\right) - \frac{\varepsilon/\mu}{4\pi\varepsilon^{4/3}\gamma g(\tau)} \right]^2, \quad (25)$$

$$K(\tau) = \frac{[\sinh(2\tau) - 2\tau]^{1/3}}{2^{1/3} \sinh \tau}. \quad (26)$$

One can check that (22) smoothly interpolates to the two-field potential derived in Ref. [18] in the large τ limit $\varepsilon^2 \cosh \tau \approx \varepsilon^2 e^\tau / 2 \approx r^3$, where r is the usual radial coordinate of the singular conifold⁷.

Having obtained the two-field F -term scalar potential $V_F(\tau, \sigma)$, the canonical inflaton can be derived from the DBI action of a mobile D3 brane moving in the full deformed conifold metric as the following integral expression;

$$\phi(\tau) = \sqrt{\frac{T_3}{6}} \varepsilon^{2/3} \int_\tau d\tau' \frac{d\tau'}{K(\tau')}. \quad (27)$$

Here, we have used the explicit deformed conifold metric given in terms of radial and angular coordinates (see, for example, Refs. [29, 31]), and one can see this definition has the asymptotic limits

$$\phi(\tau) \rightarrow \begin{cases} \sqrt{\frac{3}{2}} T_3 r, & (\tau \gg 1) \\ \frac{\sqrt{T_3}}{2^{5/6} 3^{1/6}} \varepsilon^{2/3} \tau, & (\tau \ll 1) \end{cases} \quad (28)$$

where we have used the definition $r^3 = \varepsilon^2 \cosh \tau$ to rewrite the $\tau \gg 1$ limit. The expressions of the canonical inflaton in the large and small τ limits have been used in Refs. [18] and [24], respectively.

As the deformed conifold throat is attached to a compact Calabi-Yau at some finite ultraviolet radius r_{UV} , it is important to stabilize the volume modulus σ , which controls the overall size. Within the adiabatic approximation proposed in Ref. [18], such that σ is stabilized at an instantaneous minimum as the radial coordinate τ varies, this amounts to solving the equation

$$\left. \frac{\partial(V_F + V_{\text{uplift}})(\tau, \sigma)}{\partial \sigma} \right|_{\sigma_*(\tau)} = 0. \quad (29)$$

Here, we have included the positive definite potential $V_{\text{uplift}}(\tau, \sigma) = (D_0 + D_{\text{others}})/[U(\tau, \sigma)]^2$, which is required

⁷ However, we have checked that once the volume modulus σ is stabilized in the adiabatic approximation we shall discuss next, there are deviations in resultant single field potentials, due to different radial dependence of $\sigma(\tau)$.

to uplift the total energy and to obtain a de Sitter phase. $V_{\text{uplift}}(\tau, \sigma)$ can include the first term of $V_{D3\overline{D3}}(\phi)$ given by (1) and other supersymmetry breaking sources in the bulk as encoded in $D_{\text{others}}/[U(\tau, \sigma)]^2$, which can be generated by distant $\overline{D3}$ or wrapped D7 with supersymmetry breaking world volume fluxes [32]⁸. One can also parametrize the uplifting potential by defining the uplifting ratio s as

$$s = \frac{V_{\text{uplift}}(0, \sigma_F)}{|V_F(0, \sigma_F)|}, \quad (30)$$

with σ_F being given by $\partial_\sigma V_F(0, \sigma)|_{\sigma=\sigma_F} = 0$. The distant sources are essentially needed for a small positive cosmological constant at the end of inflation after D3- $\overline{D3}$ annihilation. Combining this fact with the requirement that $s \lesssim 3$ during inflation for avoiding runaway decompactification, one can deduce that D_{others} should typically dominate over D_0 . Alternatively, one can also argue that as the distant sources are located in the unwarped region, it should naturally dominate over the $\overline{D3}$ localized at the tip of the highly warped deformed conifold [24].

Equation (29) is transcendental and is usually solved numerically. However to get a qualitative understanding, we can adopt a semi-analytic approach given in Ref. [18], where one sets the σ dependence in $U(\tau, \sigma)$ equals to large fixed value σ_0 and treat (29) as a quadratic equation of the variable $\exp[-a\sigma_*(\phi)]$. A double expansion in $1/\sigma_0$ and $\phi(\tau)$ around the tip region, such that $\phi(\tau)$ is approximated by the $\tau \ll 1$ limit of (28), then yields at leading order correction

$$\sigma_*(\phi) \approx \sigma_0 \left\{ 1 + \frac{1}{a\sigma_F} \left[\frac{1}{3} + \frac{(2/3)^{2/3} \alpha}{8n(1+\alpha)\beta} \right] \left(\frac{\phi}{M_{\text{Pl}}} \right)^2 \right\}. \quad (31)$$

In deriving the above expression we have used the approximation $a\sigma_0 \approx a\sigma_F + s/(a\sigma_F)$ given in Ref. [18]⁹. Note that we have introduced two important dimensionless parameters

$$\alpha = \frac{\varepsilon}{\mu}, \quad (32)$$

$$\beta = \sqrt{\frac{T_3}{6}} \frac{\varepsilon^{2/3}}{M_{\text{Pl}}}. \quad (33)$$

⁸ The precise $U(\tau, \sigma)$ dependence in fact varies for different distant supersymmetry breaking sources: for $\overline{D3}$ the potential $\sim U(\tau, \sigma)^{-2}$ and for D-term uplifting [32] induced by D7 carrying supersymmetry breaking flux, it is $\sim U(\tau, \sigma)^{-3}$. Here in the limit $U(\tau, \sigma) \gg 1$, we merely keep the most dominant contribution.

⁹ Let us comment on the difference between the expression for $\sigma_*(\phi)$ in Ref. [18], which was given schematically by $\sigma_*(\phi) \approx \sigma_0 [1 + b_{3/2}(\phi/M_{\text{Pl}})^{3/2}]$, and our expression (31). In Ref. [18], $V_F(\tau, \sigma)$ was calculated exclusively for the large radius, singular conifold limit. The authors of Ref. [18] then expanded in canonical inflaton $\phi \approx \sqrt{3} T_3 / 2r$ around the near tip region of deformed conifold to extract the radial dependence of the stabilized volume. Here we improved upon such calculation, using $V_F(\tau, \sigma)$ for the *entire* deformed conifold and expanding near the tip of the deformed conifold using the small radius limit of the canonical inflaton (28) to obtain the expression (31).

Geometrically, α measures the depth which D7 branes extend into deformed conifold, and β is proportional to the warp factor a_0 at the tip. Of course the analytic approximation for the stabilized volume $\sigma_*(\phi)$ only gives a qualitative understanding, and is expected to deviate from the actual behavior at large radius. For full quantitative parameter scanning how-

ever, the numerical solution to (29) can also be readily implemented.

Combining our expression for the stabilized volume $\sigma_*(\phi)$ given by (31), the potential $V_{D3\overline{D3}}(\phi) + V_{\text{stab.}}(\phi)$ for the D7 embedding (18) in the entire deformed conifold is finally given by

$$V_{D3\overline{D3}}(\phi) + V_{\text{stab.}}(\phi) = \frac{2a^2\kappa^2|A_0|^2 e^{-2a\sigma_*(\tau)}}{\{U[\tau, \sigma_*(\tau)]\}^2} |g(\tau)|^{2/n} \left\{ \frac{U[\tau, \sigma_*(\tau)]}{6} + \frac{1}{a} \left(1 - \frac{|W_0|}{|A_0|} \frac{e^{a\sigma_*(\tau)}}{[g(\tau)]^{1/n}} \right) + F(\tau) \right\} + \frac{D(\phi)}{\{U[\tau, \sigma_*(\tau)]\}^2}, \quad (34)$$

$$D(\phi) = D_0 \left(1 - \frac{27D_0}{64\pi^2\phi^4} \right) + D_{\text{others}}. \quad (35)$$

Here, we should regard the radial coordinate τ to be an implicit function of the canonical inflaton ϕ given by (27). In addition, as shown in Ref. [24] the residual angular isometry directions become degenerate along the trajectory (21). Therefore D3- $\overline{D3}$ separation $|\mathbf{y} - \bar{\mathbf{y}}|$ is purely radial and proportional to the canonical inflaton $\phi(\tau)$ for the entire deformed conifold. In Fig. 1, we show the plot of the potential (34) with the parameters given by Case 1 of Table I.

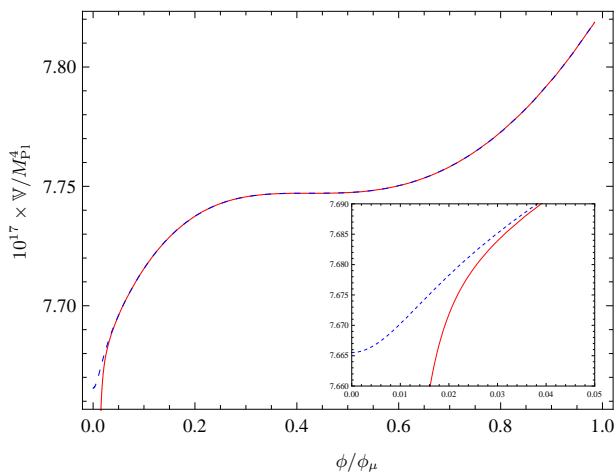


FIG. 1: The plot of the potential (34) as a function of ϕ/ϕ_μ , with $\phi_\mu^2 \equiv 3T_3/2(2\mu^2)^{2/3}$. The parameters are set the same as Case 1 of Table I. We show two extreme cases of $D(\phi)$: either it is completely dominated by the Coulombic interaction (solid line) or by the distant sources (dotted line). Note that the difference becomes only noticeable at the region very close to the tip, as shown in the inset, which magnifies the potential in this region. This implies inflation only ends when ϕ approaches close to the tip, even if the potential is highly curved by the Coulombic term: in the case shown here, $\phi_e \approx 0.0105\phi_\mu$, meanwhile the “potential” slow-roll parameter with higher order corrections [33] gives $\phi_e \approx 0.0700\phi_\mu$. Note that $|\eta| \equiv |M_{\text{Pl}}^2 \nabla''/\nabla| = 1$ well before this point, at $\phi \approx 0.324\phi_\mu$.

Let us conclude this section by revisiting the η problem discussed in Ref. [18], now with the potential (34) valid in the

region near the tip with the small field canonical inflaton given in (28) and the stabilized volume (31). After some expansions, we can obtain

$$\frac{V_{D3\overline{D3}}(\phi) + V_{\text{stab.}}(\phi)}{V_{D3\overline{D3}}(0) + V_{\text{stab.}}(0)} \approx 1 + \frac{\phi^2}{3M_{\text{Pl}}^2} \left[1 + \mathcal{O}\left(\frac{1}{\sigma_0}\right) \right] + \mathcal{O}(\phi^4). \quad (36)$$

Notice that the dependence of the gaugino condensate on the mobile D3 brane position *does* give corrections to the inflaton mass in the near tip region. However, such corrections are suppressed by the large stabilized volume σ_0 , and are insufficient to give small inflaton mass. Thus, η remains of order one¹⁰. This is in fact consistent with the analysis in Ref. [18] using the singular conifold approximation, that the inflection point $\eta = 0$ only appears at some intermediate radius¹¹.

Parametrization of the bulk effects

To account for the ultraviolet physics arising from attaching the warped throat to a compact Calabi-Yau, a useful parametrization of the leading corrections was given in Ref. [15]. The authors employed gauge/string correspondence for the warped deformed conifold (see, for example, Refs. [29, 31]), where the position of the mobile D3 is identified with the Coulomb branch vacuum expectation value of the dual field theory. In such a holographic formulation, the symmetry breaking bulk effects can be encoded by coupling a field theory operator \mathcal{O}_Δ of scaling dimension Δ to its dual bulk mode and a perturbation to inflaton ϕ potential is gener-

¹⁰ Notice that on the other hand $|\varepsilon| \ll 1$, as we do not have trans-Planckian field displacement $\Delta\phi/M_{\text{Pl}} \ll 1$.

¹¹ Notice that the analysis here is accurate for the near tip region. The required cancellation term $\propto \phi^{3/2}$ for obtaining inflection point, only appears when the large radius canonical inflaton (28) and the associated stabilized volume expression are substituted in the derivation.

ated as

$$\Delta V = -c_\Delta a_0^4 T_3 \left(\frac{\phi}{\phi_{UV}} \right)^\Delta. \quad (37)$$

Here $\phi_{UV} = \sqrt{3T_3/2} r_{UV}$ and r_{UV} is the radius at which the deformed conifold throat joins the compact Calabi-Yau. The positive constant c_Δ depends on the specific distant fluxes or brane configurations¹². Varying its value allows us to parametrize our ignorance about this information. The normalization of $a_0^4 T_3$ in (37) comes from the estimated energy required to move the mobile D3 from its supersymmetric minimum to the four cycle moduli stabilizing D7 wraps. This is proportional to the height of the anti de Sitter potential barrier which in our more detailed setup should be identified explicitly with $|V_F(0, \sigma_F)|$.

There can in fact be whole series of perturbations of the form given in (37). However the two leading contributions come from the lowest chiral multiplet of dimension $3/2$, $\mathcal{O}_{3/2}$, and the lowest non-chiral multiplet of dimension 2, \mathcal{O}_2 . For our case, the bulk potential as denoted in (2) is then given by

$$V_{\text{bulk}}(\phi) = -|V_F(0, \sigma_F)| \left[c_{3/2} \left(\frac{\phi}{\phi_{UV}} \right)^{3/2} + c_2 \left(\frac{\phi}{\phi_{UV}} \right)^2 \right]. \quad (38)$$

One can of course include other higher dimensional operators in $V_{\text{bulk}}(\phi)$. The terms above are merely to illustrate the importance of bulk physics in our later sample parameter scanings¹³. However, one should note that when more than one $(\phi/\phi_{UV})^\Delta$ is turned on in (38), there are generally additional angular perturbations. This comes from the fact that individual coefficient c_Δ is obtained from integrating out complicated angular dependences. When more than one c_Δ are involved, it is generally not possible to perform such integrating out¹⁴.

CONSTRAINING PARAMETER SPACE: MICROSCOPIC AND OBSERVATIONAL

Microscopic constraints

Let us first list out the explicit parameters specifying the total single field inflaton potential $\mathbb{V}(\phi) = V_{D3\bar{D}3}[\phi, \sigma_*(\phi)] + V_{\text{stab.}}[\phi, \sigma_*(\phi)] + V_{\text{bulk}}[\phi, \sigma_*(\phi)]$; they are

$$\{n, |A_0|, |W_0|, s, \epsilon, \mu, c_{3/2}, c_2\}. \quad (39)$$

¹² To be specific, c_Δ used here only incorporate strictly bulk effects. This is in contrast with Ref. [15], where the c_Δ coefficients there can receive *both* local and bulk contributions.

¹³ In Ref. [34], an earlier attempt to perform parameter scanning using (38) is given.

¹⁴ We are grateful to Daniel Baumann for pointing this out to us.

Here, we have used the F -term flatness condition $D_\sigma W|_{\sigma_F} = 0$,

$$e^{a\sigma_F} = \frac{|A_0|}{|W_0|} \left(1 + \frac{2}{3} a\sigma_F \right) (1 + \alpha)^{1/n}, \quad (40)$$

to exchange $|W_0|$ for σ_F . From the perspective of Kähler moduli stabilization, σ_F should be regarded as a derived parameter, which is obtained as soon as the hierarchy between $|A_0|$ and $|W_0|$ is specified¹⁵. Before comparing with the observational data, there are additional microscopic requirements that need to be satisfied a priori. Here, we list them below.

- The string coupling g_s should be small, i.e. $g_s \ll 1$ to ignore the string loop corrections to the supergravity action. The physical radius of the three sphere at the tip of deformed conifold is $g_s M \alpha'$; thus, we also need $g_s M \gg 1$ [29].
- The ultraviolet cutoff r_{UV} should be large such that $r_{UV}/l_s \gg 1$ for valid supergravity solution. This sets the upper bound on the displacement for ϕ , hence the total number of e -folds. Moreover, the unit of five form flux $N = KM$ controlling the size of conifold needs to be large for the supergravity approximation to be valid. These geometric requirements combine to give a strong bound on the tensor-to-scalar ratio r [35],

$$\frac{4}{N} \gtrsim \left(\frac{\phi_{UV}}{M_{\text{Pl}}} \right)^2 \gtrsim 100 \times r, \quad (41)$$

where the \gtrsim sign is to indicate that bulk volume can also give significant contribution to V_6^w . This can be obtained from the relation between the four dimensional reduced Planck mass M_{Pl} and the warped volume V_6^w of the compact six manifold. Given $N \gg 1$, the inequality (41) implies that warped brane inflation yields negligible tensor-to-scalar ratio.

- The stabilized volume modulus σ_F should also be at large values for the α' corrections to be suppressed. This can be ensured by tuning the bulk flux to generate a large hierarchy between $|A_0|$ and $|W_0|$, i.e. $|A_0|/|W_0| \gg 1$, since $a = 2\pi/n$ is typically smaller than 1 so that large σ_F can be readily produced. To avoid the back-reaction of D7 branes on the deformed conifold, however, n should also be such that $n/M \ll 1$. This ensures that the resultant geometry is smooth at the end of duality cascade, rather than cascading into singular conifold throat.

¹⁵ Furthermore, in this paper, we shall consider the configuration where moduli stabilizing D7 brane is sufficiently far away from the tip of the deformed conifold. Therefore the term $1 + \alpha$ with $\alpha = \epsilon/\mu \ll 1$ in (40) only gives insignificant shift in σ_F .

- Finally, the uplifting ratio s is bounded within the range $1 \leq s \leq O(3)$ to ensure a small positive cosmological constant at the end of inflation. The upper bound here arises from preventing runaway decompactification. Such requirement effectively couples the scale of $|V_F|$ and the scale of the uplifting term(s) $V_{\text{uplift}}(\phi)$.

Comparison with observations

In this section we shall first consider some generic features of the inflaton potential (2) with $c_{3/2} = c_2 = 0$, i.e. involving only $V_{D_3\overline{D}_3}(\phi) + V_{\text{stab.}}(\phi)$ given by (34). In particular, we discuss which parameters listed in (39) have more impact on the overall scale or the detailed shape of the inflaton potential, as this is useful for an efficient full parameter space scanning. Next, we shall present some sample parameter sets to demonstrate that $V_{D_3\overline{D}_3}(\phi) + V_{\text{stab.}}(\phi)$ can indeed yield observationally consistent results. Such scanning for our complete potential is in line with the existing literature [16, 17]. Finally, we shall scan the perturbations due to $V_{\text{bulk}}(\phi)$ on these observationally consistent local potential $V_{D_3\overline{D}_3}(\phi) + V_{\text{stab.}}(\phi)$, and demonstrate that bulk contributions generically need to be highly fine-tuned to preserve such results.

Let us first consider the amplitude of the power spectrum of the curvature perturbation $\mathcal{P}_{\mathcal{R}}$ and the corresponding spectral index $n_{\mathcal{R}}$, which are tightly constrained by recent cosmological observations [2, 3]. On the largest observable scales the slow-roll approximation holds at a good enough accuracy (see later discussion), we can express them as

$$\mathcal{P}_{\mathcal{R}} = \frac{\mathbb{V}}{24\pi^2\epsilon M_{\text{Pl}}^4} = (2.41 \pm 0.22) \times 10^{-9}, \quad (42)$$

$$n_{\mathcal{R}} = 1 - 6\epsilon + 2\eta = 0.963 \pm 0.028, \quad (43)$$

at 95% confidence level. Here, (42) and (43) are evaluated at ϕ_{CMB} , the value of the canonical inflaton at the CMB scale, and should be determined by integrating backwards 60 e -folds¹⁶ from the end of inflation. The inflationary scale is expected to be approximately constant around the CMB scale, and, in particular, for our model, it is expected to occur near the ‘‘inflection point’’ where the majority of e -folds is generated. Explicitly, the combination

$$(s-1)|V_F(0, \sigma_F)| \approx (s-1) \frac{a^2 |A_0|^2 e^{-2a\sigma_F}}{3M_{\text{Pl}}^2 (2\sigma_F)} \approx \mathbb{V}(\phi_{\text{CMB}}) \quad (44)$$

largely sets the overall scale of inflation in our model. The deviation from (44) due to the motion of mobile D3 is essentially a small fluctuation around it. If the energy associated

with the inflaton is too large, this would in fact lead to runaway decompactification [37]. The slow-roll parameter ϵ is also small around the CMB scale, but it varies more rapidly than $\mathbb{V}(\phi)$. We therefore conclude to obtain an observationally consistent value of (42), it is easier to fix the combination (44) which sets the overall scale, then vary other parameters such as ϵ and μ , which affect the shape of $\mathbb{V}(\phi)$ around ϕ_{CMB} .

It is also worth noting that while the uplifting ratio s or $V_{\text{uplift}}(\phi)$ is fixed, one can still vary the ratio between the distant uplifting ($\propto D_{\text{others}}$) and contribution from \overline{D}_3 at the tip of ($\propto D_0$). This also varies the D3- \overline{D}_3 Coulombic attraction in (1). However, as such highly warped attraction only becomes significant near the tip region, it is important to use the full scalar potential (34) to study any change in the trajectory. Furthermore, at the relatively large distance where the CMB scale lies, the Coulombic attraction is effectively absent. The variation of D_0/D_{others} therefore should not affect significantly the observational predictions¹⁷. This is indeed the case as illustrated in Fig. 1 and Table I.

Now we would like to present some sample parameter scanings for $V_{D_3\overline{D}_3}(\phi) + V_{\text{stab.}}(\phi)$. The strategy is that we shall further systematically fix the parameters $n, |A_0|, |W_0|$ and s to some appropriate fiducial values by hand. This allows us to roughly fix the overall scale of the inflaton potential following (44). We then generate a range of observationally consistent parameter sets by scanning in ϵ - μ or equivalently α - β plane.

Let us briefly describe how the fiducial values for these other parameters are chosen. The number of probe D7s n can first be fixed to be sufficiently small. This is because n appears mostly with σ_* or in $[g(\tau)]^{1/n}$. With $\alpha \cosh(\tau/2) < 1$ and $\sigma_F \gg 1$, the dependence of the inflaton potential on n is insignificant comparing with other parameters. To fix the values of $|A_0|, |W_0|$ and s , as mentioned earlier that their relative sizes are fixed by compactification constraints (40), we need to set the ratio $|A_0|/|W_0|$ large to ensure the volume modulus is fixed at large value σ_F . For the actual value of $|A_0|$, we note that as $|A_0|$ is related to the dynamical scale Λ at which gaugino condensation takes place [17], therefore it is necessary to have $|A_0|^{1/3} \sim \Lambda \leq M_{\text{Pl}}$. To fix the uplifting ratio s , the resultant cosmological constant should be small and positive at the end of inflation, but not necessarily at our current value as, for example, there can be further dynamical processes, e.g. topological changes after inflation, which can change its value. The specific numerical values for $\{n, |A_0|, |W_0|, s\}$ used in our scanning are given in Table I.

With the full inflaton potential given by (34) and (38), we can *exactly* solve the system and subsequently identify where inflation ends, i.e. $\epsilon = 1$. This is most easily done by solving, instead of the Friedmann equation, the Hamilton-Jacobi

¹⁶ There exists some level of uncertainty on exactly when the perturbation on the largest observable scales is generated. Depending on the detail of the model, the corresponding e -fold is supposed to lie between 50 and 60 [36]. But provided that the curvature power spectrum is nearly scale invariant it does not cause too significant differences. Thus in the remaining text we evaluate $\mathcal{P}_{\mathcal{R}}$ and $n_{\mathcal{R}}$ at 60 e -folds before the end of inflation.

¹⁷ It is in principle possible to finely tune the CMB scale to small radius [17], but there one should again use the full potential valid for that region (34) to study the effects of varying D_0/D_{others} on the trajectory.

equation

$$2M_{\text{Pl}}^4[H'(\phi)]^2 - 3M_{\text{Pl}}^2[H(\phi)]^2 + \mathbb{V}(\phi) = 0. \quad (45)$$

We can thus calculate the *exact* number of e -folds \mathcal{N}_e given by

$$\mathcal{N}_e(\phi) = M_{\text{Pl}}^{-1} \int_{\phi_e}^{\phi} \frac{d\phi}{\sqrt{2\epsilon}}, \quad (46)$$

with ϵ defined as (3) and ϕ_e given by solving (45), and subsequently identify ϕ_{CMB} where $\mathcal{N}_e(\phi_{\text{CMB}}) = 60$. Note that for ϕ_e , we explicitly consider two limiting cases, where the uplifting is exclusively by the distant sources or by the warped $\overline{\text{D3}}$. As mentioned earlier and checked in our scanings that $\epsilon \ll 1$ until the tip of deformed conifold for distant uplifting, thus $\phi_e = 0$ in this case. Whereas for warped $\overline{\text{D3}}$, ϕ_e can also be determined at a small radius by solving (3). Essentially we expect that the end point ϕ_e will vary continuously as we dial between the two limit cases. Furthermore, at any viable ϕ_{CMB} the potential is very flat so that $|\eta| \ll 1$, we therefore make use of the simplified slow-roll formulae (42) and (43) to estimate $\mathcal{P}_{\mathcal{R}}$ and $n_{\mathcal{R}}$ respectively, instead of solving the perturbation equations mode by mode.

In Table I, we present three sets of α and β , which give similar predictions on $\mathcal{P}_{\mathcal{R}}$ and $n_{\mathcal{R}}$ for $V_{D3\overline{D3}}(\phi) + V_{\text{stab.}}(\phi)$. The values of W_0 and A_0 are the same in both Cases 1 and 2. The scanned results suggest that locally there exists a region of degeneracies in α - β plane with the other parameters fixed, as explicitly demonstrated in the lower panels of Fig. 2. Furthermore, if the other parameters are allowed to vary, we can produce similar prediction in an even wider range of parameter sets. A sample parameter set with different $|A_0|$ and $|W_0|$ is presented as Case 3 in Table I. Note that from Fig. 2, a fractional change of $O(1)\%$ in either α or β can easily move the values of $\mathcal{P}_{\mathcal{R}}$ and $n_{\mathcal{R}}$ to observationally inconsistent regimes. Here, we have scanned only the vicinity of a given $\{\alpha, \beta\}$, and it is not entirely clear (although suggestive) such $O(1)\%$ tuning in α - β plane holds for a wider range. It would be interesting to return to this issue in a more complete scanning in the future.

Bulk effects scanning

Having presented a range of the observationally consistent parameter sets for $V_{D3\overline{D3}}(\phi) + V_{\text{stab.}}(\phi)$, we shall now consider the perturbations on them, due to the unknown bulk physics parametrized by $V_{\text{bulk}}(\phi)$ (38). In particular, for the local inflection point based inflationary trajectories, we shall perform a sample scanning in the $c_{3/2}$ - c_2 plane to demonstrate that they typically need to be of order 10^{-8} - 10^{-9} to preserve consistent observational predictions.

	$ W_0 $	$ A_0 $	α	β	$\mathcal{P}_{\mathcal{R}} \times 10^9$	$n_{\mathcal{R}}$
Case 1	2.92485×10^{-6}	0.0085	1/200	1/508	2.66644	0.933109
					2.49420	0.932009
Case 2	2.92485×10^{-6}	0.0085	1/100	1/320	2.59208	0.934267
					2.42615	0.933175
Case 3	3.3×10^{-6}	0.066	1/100	1/350	2.36186	0.934743
					2.19847	0.933838

TABLE I: Three sets of parameters that give the viable values of $\mathcal{P}_{\mathcal{R}}$ and $n_{\mathcal{R}}$. We have fixed $n = 8$ and $s = 1.07535$ for all the cases. The values of the tensor-to-scalar ratio $r = 16\epsilon$ and the non-linear parameter $f_{\text{NL}} = O(\epsilon, \eta)$ are unobservably small and hence we do not present them here. The first line of each case corresponds to the complete domination of the distant sources, while the second to that of the Coulombic interaction. Note that as shown in the first two cases, with a given set of $n, s, |W_0|$ and $|A_0|$, a different combination of α and β yields similar values of $\mathcal{P}_{\mathcal{R}}$ and $n_{\mathcal{R}}$. Also, in the last case with another set of $|W_0|, |A_0|, \alpha$ and β we can find observationally consistent values of $\mathcal{P}_{\mathcal{R}}$ and $n_{\mathcal{R}}$.

For numerical purpose, we slightly recast (38) as

$$V_{\text{bulk}}(\phi) = -|V_F(0, \sigma_F)| \times \left\{ c'_{3/2} \alpha \left[\int_{\tau} d\tau' K(\tau') \right]^{3/2} + c'_2 \alpha^{4/3} \left[\int_{\tau} d\tau' K(\tau') \right]^2 \right\}. \quad (47)$$

In the above we have used

$$\frac{\phi}{\phi_{\text{UV}}} = \frac{\phi_{\mu}/\phi_{\text{UV}}}{2^{1/3} \cdot 3} \alpha^{2/3} \int_{\tau} d\tau' K(\tau'), \quad (48)$$

with $\phi_{\mu}/\phi_{\text{UV}} \lesssim 1$ being a number (This is denoted as Q_{μ}^{-1} in Refs. [18, 24]) and various order one numerical factors are absorbed into a newly defined constant c'_{Δ} . Hereafter, we shall drop this prime notation. In general, as $V_{D3\overline{D3}}(\phi)$ yields a delicate inflection point based inflation, we expect the value of c_{Δ} needs to be finely tuned. In Table II we show a summary of the effects of V_{bulk} .

Specifically, from Table II, we can see that a very slight disturbance of the bulk effects of magnitude 10^{-9} - 10^{-8} for both $c_{3/2}$ and c_2 can push the otherwise viable predictions into the regions beyond $2\text{-}\sigma$ errors. As V_{bulk} is negative definite, it pushes down the inflaton potential further so that the previously flat region becomes flatter or is even changed into a local minimum. Naturally the amplitude of $\mathcal{P}_{\mathcal{R}}$ increases, while $n_{\mathcal{R}}$ deviates further from 1 as the value of the coefficients $c_{3/2}$ and c_2 get larger. These tendencies are clearly shown in Table II. Occasionally V_{bulk} can improve the relevant predictions to be closer to the current observations. For example, in Case 3, the bulk terms move the value of $\mathcal{P}_{\mathcal{R}}$ to the central value of the observationally allowed region and leave $n_{\mathcal{R}}$ more or less the same with small $c_{3/2}$ and c_2 . One may thus hope that by adding $V_{\text{bulk}}(\phi)$ to an unviable $V_{D3\overline{D3}}(\phi) + V_{\text{stab.}}(\phi)$, observationally consistent results can be obtained. However, we expect in general $c_{3/2}$ or c_2 need to be of order 10^{-8} - 10^{-9} to achieve such objective.

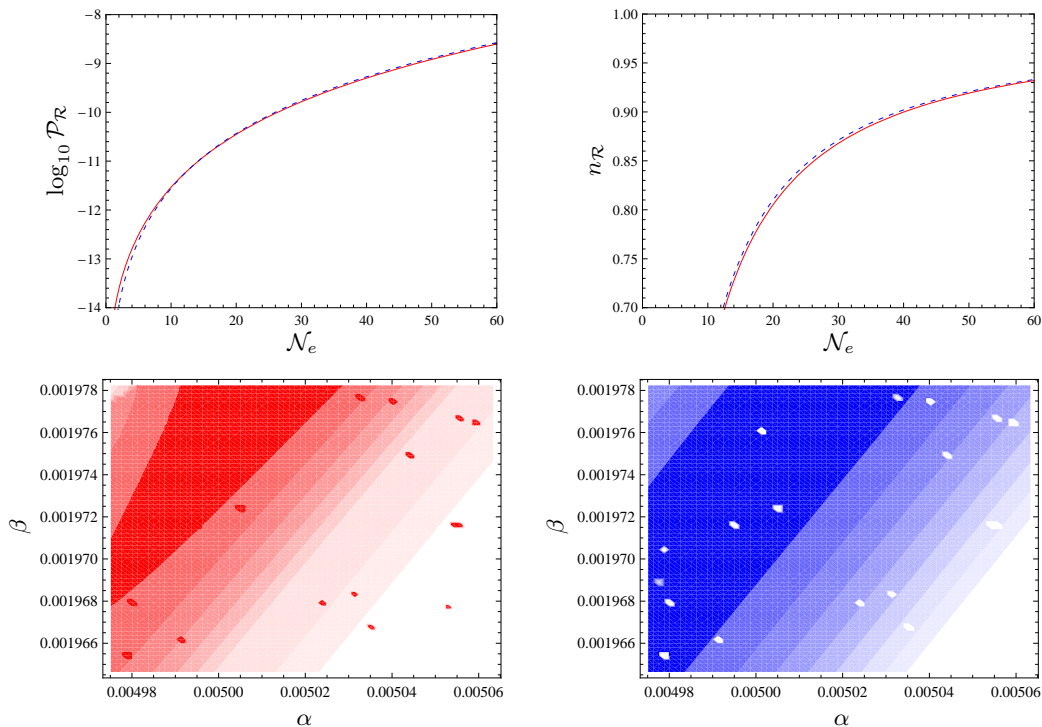


FIG. 2: (Upper panels) the plots of (left panel) $\log_{10} \mathcal{P}_{\mathcal{R}}$ and (right panel) $n_{\mathcal{R}}$ as functions of \mathcal{N}_e , and (lower panels) the contour plots of (left panel) $\mathcal{P}_{\mathcal{R}}$ and (right panel) $n_{\mathcal{R}}$ in the α - β plane for Case 1 given in Table I. In the upper panels we show the two extreme cases where $D(\phi)$ given by (35) is completely dominated by either the Coulombic interaction (solid line) or the distant sources (dotted line). Meanwhile, in the lower panels we only present the case with the distant sources completely dominating. In the contour plot of $\mathcal{P}_{\mathcal{R}}$, the contours denote $2.5, 2.6, 2.7, 2.8, 2.9, 3.0, 3.5, 4.0 \times 10^{-9}$ from the innermost line. Likewise we have set $0.9325, 0.9300, 0.9275, 0.9250, 0.9225, 0.9200, 0.9175, 0.9150$ for the contour plot of $n_{\mathcal{R}}$. The dots in the contour plots are numerical glitches. We have obtained qualitatively the same contour plots when the Coulombic interaction is dominating instead, with the deep colored region a bit enlarged ($\mathcal{P}_{\mathcal{R}}$) and shrunk ($n_{\mathcal{R}}$).

DISCUSSIONS

In this paper, we have discussed in detail the inflaton potential governing the motion of a mobile D3 in the entire warped deformed conifold. In particular, we have included both the effects of moduli stabilization and other bulk physics. We then have performed some sample scanings to demonstrate that without the bulk perturbations, there can be significant degeneracies in the conifold deformation parameter ε and the D7 embedding parameter μ for producing observationally consistent predictions. However, as the bulk perturbations are included, we have explicitly shown that their magnitudes need to be 10^{-8} - 10^{-9} to preserve the observationally consistent parameter sets¹⁸. The results presented here provide the beginning systematic steps towards a complete brane scanning in

the warped throat, and, in particular, highlight the importance of the bulk effects.

It would be very interesting to follow the steps outlined here and perform a full scanning over the parameters listed in (39). This clearly requires intensive computational undertakings. However given the rich parameter space and the degeneracies we have shown in the sample scanings, barring the observation of the primordial gravitational waves, it is likely that there remain significant regions in the parameter space for the warped brane inflation to match the future data. Moreover, a variant of the inflation model presented here is recently proposed in Ref. [38]. In such a construction the gravitino mass $m_{3/2}$ can be made smaller than the Hubble scale H , hence circumventing the phenomenological bound given in Ref. [37]. It would clearly be interesting to generalize the analysis here and scan the parameter space for such variant, and search for an explicit example of a parameter set that gives TeV scale gravitino mass and observationally consistent cosmological predictions.

¹⁸ An obviously interesting question would be whether the smallness of bulk perturbation coefficients c_A really constitutes a significant fine-tuning, or they are just tied to the choice of having inflection point inflation in the throat. To answer this question fully, we believe it requires better than our current understanding of UV physics and beyond the scope of investigations here.

			$c_{3/2}$				c_2			
			10^{-9}	10^{-8}	10^{-7}	10^{-6}	10^{-9}	10^{-8}	10^{-7}	10^{-6}
Case 1	Distant sources	$\mathcal{P}_{\mathcal{R}} \times 10^9$	2.71386	3.17635	13.7483	26670.1	2.74701	3.58118	37.8218	0.0559217*
		$n_{\mathcal{R}}$	0.932540	0.927506	0.883792	0.657621	0.932149	0.923750	0.856258	0.552413
Case 1	Coulomb interaction	$\mathcal{P}_{\mathcal{R}} \times 10^9$	2.53682	2.95080	11.9644	11348.2	2.56657	3.31098	31.2301	0.0138777*
		$n_{\mathcal{R}}$	0.931448	0.926480	0.883233	0.657668	0.931062	0.922766	0.855908	0.552458
Case 2	Distant sources	$\mathcal{P}_{\mathcal{R}} \times 10^9$	2.63754	3.08041	13.0733	22761.8	2.66847	3.45614	34.6474	0.0399836*
		$n_{\mathcal{R}}$	0.933704	0.928724	0.885438	0.661093	0.933327	0.925100	0.858794	0.559159
Case 2	Coulomb interaction	$\mathcal{P}_{\mathcal{R}} \times 10^9$	2.46750	2.86903	11.5801	10664.9	2.49564	3.20800	29.4348	0.01153290*
		$n_{\mathcal{R}}$	0.932613	0.927646	0.884425	0.659278	0.932238	0.924026	0.857777	0.556756
Case 3	Distant sources	$\mathcal{P}_{\mathcal{R}} \times 10^9$	2.40944	2.87842	14.8411	70552.3	2.44157	3.27915	43.8420	0.186355*
		$n_{\mathcal{R}}$	0.934097	0.928393	0.879688	0.636830	0.933668	0.924284	0.850560	0.528232
Case 3	Coulomb interaction	$\mathcal{P}_{\mathcal{R}} \times 10^9$	2.24107	2.65907	12.7450	27115.1	2.26982	3.01367	35.5661	0.0400323*
		$n_{\mathcal{R}}$	0.933199	0.927564	0.879325	0.636940	0.932776	0.923498	0.850383	0.528320

TABLE II: The effects of the bulk terms for each case of Table I. For definiteness, we have turned on either $c_{3/2}$ or c_2 , not both of them at the same time. This was also needed to ensure that we can avoid additional angular perturbations mentioned earlier in the main text. Also note that the values of $\mathcal{P}_{\mathcal{R}}$ when $c_2 = 10^{-6}$, denoted by a superscript * in the last column, are bare ones and the factor of 10^9 is *not* multiplied.

Acknowledgement

We thank Gary Shiu for collaboration and discussions at the early stage of this project. We are also grateful to Ana Achúcarro, Daniel Baumann, James Cline, Shamit Kachru, Gonzalo Palma, Fernando Quevedo, Koenraad Schalm and Bret Underwood for comments and suggestions. HYC appreciates the hospitality of Stanford Institute for Theoretical Physics, where part of this work was conducted. The work of HYC is supported in part by NSF CAREER Award No. PHY-0348093, DOE grant DE-FG-02-95ER40896, a Research Innovation Award and a Cottrell Scholar Award from Research Corporation, and a Vilas Associate Award from the University of Wisconsin. JG is partly supported by the Korea Research Foundation Grant KRF-2007-357-C00014 funded by the Korean Government at the early stage of this work, and is currently supported in part by a VIDi and a VICI Innovative Research Incentive Grant from the Netherlands Organisation for Scientific Research (NWO).

- E. Silverstein, *Gen. Rel. Grav.* **40** (2008) 565 [arXiv:0710.2951 [hep-th]].
- [5] [Planck Collaboration], arXiv:astro-ph/0604069.
- [6] <http://cmbpol.uchicago.edu/> ; http://www.astro.caltech.edu/~lgg/spider_front.htm
- [7] <http://nasascience.nasa.gov/missions/jdem/>
- [8] <http://sci.esa.int/science-e/www/object/index.cfm?fobjectid=42266>
- [9] G. R. Dvali and S. H. H. Tye, *Phys. Lett. B* **450**, 72 (1999) [arXiv:hep-ph/9812483].
- [10] S. Kachru, R. Kallosh, A. Linde, J. M. Maldacena, L. P. McAllister and S. P. Trivedi, *JCAP* **0310**, 013 (2003) [arXiv:hep-th/0308055].
- [11] S. Gukov, C. Vafa and E. Witten, *Nucl. Phys. B* **584** (2000) 69 [Erratum-ibid. B **608** (2001) 477] [arXiv:hep-th/9906070].
- [12] S. B. Giddings, S. Kachru and J. Polchinski, *Phys. Rev. D* **66** (2002) 106006 [arXiv:hep-th/0105097] ; S. Kachru, R. Kallosh, A. Linde and S. P. Trivedi, *Phys. Rev. D* **68**, 046005 (2003) [arXiv:hep-th/0301240].
- [13] P. Candelas and X. C. de la Ossa, *Nucl. Phys. B* **342**, 246 (1990).
- [14] A. Ceresole, G. Dall'Agata, R. D'Auria and S. Ferrara, *Phys. Rev. D* **61**, 066001 (2000) [arXiv:hep-th/9905226].
- [15] D. Baumann, A. Dymarsky, S. Kachru, I. R. Klebanov and L. McAllister, *JHEP* **0903**, 093 (2009) [arXiv:0808.2811 [hep-th]].
- [16] R. Bean, S. E. Shandera, S. H. Henry Tye and J. Xu, *JCAP* **0705** (2007) 004 [arXiv:hep-th/0702107] ; S. E. Shandera and S. H. Tye, *JCAP* **0605** (2006) 007 [arXiv:hep-th/0601099] ; L. Lorenz, J. Martin and C. Ringeval, *JCAP* **0804**, 001 (2008) [arXiv:0709.3758 [hep-th]].
- [17] L. Hoi and J. M. Cline, *Phys. Rev. D* **79**, 083537 (2009) [arXiv:0810.1303 [hep-th]].
- [18] D. Baumann, A. Dymarsky, I. R. Klebanov and L. McAllister, *JCAP* **0801** (2008) 024 [arXiv:0706.0360 [hep-th]].
- [19] C. P. Burgess, J. M. Cline, K. Dasgupta and H. Firouzjahi, *JHEP* **0703**, 027 (2007) [arXiv:hep-th/0610320].
- [20] A. Krause and E. Pajer, *JCAP* **0807** (2008) 023 [arXiv:0705.4682 [hep-th]].

* Electronic address: hchen46@wisc.edu

† Electronic address: jgong@lorentz.leidenuniv.nl

- [1] A. H. Guth, *Phys. Rev. D* **23**, 347 (1981) ; A. D. Linde, *Phys. Lett. B* **108**, 389 (1982) ; A. Albrecht and P. J. Steinhardt, *Phys. Rev. Lett.* **48**, 1220 (1982).
- [2] M. Tegmark *et al.* [SDSS Collaboration], *Phys. Rev. D* **74**, 123507 (2006) [arXiv:astro-ph/0608632] ;
- [3] E. Komatsu *et al.* [WMAP Collaboration], arXiv:0803.0547 [astro-ph].
- [4] R. Kallosh, *Lect. Notes Phys.* **738** (2008) 119 [arXiv:hep-th/0702059] ; J. M. Cline, arXiv:hep-th/0612129 ; C. P. Burgess, *PoS P2GC* (2006) 008 [Class. Quant. Grav. **24** (2007) S795] [arXiv:0708.2865 [hep-th]]. L. McAllister and

- [21] G. German, G. G. Ross and S. Sarkar, Nucl. Phys. B **608**, 423 (2001) [arXiv:hep-ph/0103243].
- [22] D. H. Lyth and D. Wands, Phys. Lett. B **524**, 5 (2002) [arXiv:hep-ph/0110002] ; T. Moroi and T. Takahashi, Phys. Lett. B **522**, 215 (2001) [Erratum-ibid. B **539**, 303 (2002)] [arXiv:hep-ph/0110096].
- [23] K. Y. Choi, J. O. Gong and D. Jeong, JCAP **0902**, 032 (2009) [arXiv:0810.2299 [hep-ph]].
- [24] H. Y. Chen, J. O. Gong and G. Shiu, JHEP **0809**, 011 (2008) [arXiv:0807.1927 [hep-th]].
- [25] O. DeWolfe and S. B. Giddings, Phys. Rev. D **67**, 066008 (2003) [arXiv:hep-th/0208123].
- [26] G. Shiu, G. Torroba, B. Underwood and M. R. Douglas, JHEP **0806**, 024 (2008) [arXiv:0803.3068 [hep-th]] ; M. R. Douglas and G. Torroba, JHEP **0905**, 013 (2009) [arXiv:0805.3700 [hep-th]] ; A. R. Frey, G. Torroba, B. Underwood and M. R. Douglas, JHEP **0901**, 036 (2009) [arXiv:0810.5768 [hep-th]] ; F. Marchesano, P. McGuirk and G. Shiu, JHEP **0904**, 095 (2009) [arXiv:0812.2247 [hep-th]].
- [27] S. B. Giddings and A. Maharana, Phys. Rev. D **73**, 126003 (2006) [arXiv:hep-th/0507158].
- [28] D. Baumann, A. Dymarsky, I. R. Klebanov, J. M. Maldacena, L. P. McAllister and A. Murugan, JHEP **0611**, 031 (2006) [arXiv:hep-th/0607050] ; O. J. Ganor, Nucl. Phys. B **499** (1997) 55 [arXiv:hep-th/9612077] ; M. Berg, M. Haack and B. Kors, Phys. Rev. D **71**, 026005 (2005) [arXiv:hep-th/0404087].
- [29] I. R. Klebanov and M. J. Strassler, JHEP **0008** (2000) 052 [arXiv:hep-th/0007191].
- [30] S. Kuperstein, JHEP **0503**, 014 (2005) [arXiv:hep-th/0411097].
- [31] C. P. Herzog, I. R. Klebanov and P. Ouyang, arXiv:hep-th/0108101 ; C. P. Herzog, I. R. Klebanov and P. Ouyang, arXiv:hep-th/0205100.
- [32] C. P. Burgess, R. Kallosh and F. Quevedo, JHEP **0310**, 056 (2003) [arXiv:hep-th/0309187].
- [33] J. O. Gong and E. D. Stewart, Phys. Lett. B **510**, 1 (2001) [arXiv:astro-ph/0101225].
- [34] A. Ali, R. Chingangbam, S. Panda and M. Sami, Phys. Lett. B **674**, 131 (2009) [arXiv:0809.4941 [hep-th]].
- [35] D. H. Lyth, Phys. Rev. Lett. **78** (1997) 1861 [arXiv:hep-ph/9606387] ; D. Baumann and L. McAllister, Phys. Rev. D **75** (2007) 123508 [arXiv:hep-th/0610285].
- [36] A. R. Liddle and S. M. Leach, Phys. Rev. D **68**, 103503 (2003) [arXiv:astro-ph/0305263] ; L. Alabidi and D. H. Lyth, JCAP **0605**, 016 (2006) [arXiv:astro-ph/0510441].
- [37] R. Kallosh and A. Linde, JHEP **0412**, 004 (2004) [arXiv:hep-th/0411011].
- [38] H. Y. Chen, L. Y. Hung and G. Shiu, JHEP **0903**, 083 (2009) [arXiv:0901.0267 [hep-th]].